On Dual Actuation in Atomic Force Microscopes

Khalid El Rifai, Osamah El Rifai, and Kamal Youcef-Toumi
77 Massachusetts Ave Room 3-348, Cambridge MA 02139
elrifai@mit.edu,osamah@mit.edu, youcef@mit.edu

Abstract

In this paper, the problem of dual actuation in the atomic force microscope (AFM) is analyzed. The use of two actuators to balance the trade-off between bandwidth, range, and precision has been recently extended to nano-positioning systems. Despite existing demands, this concept undergoes fundamental limitations towards its extension to AFMs. This is attributed to the non-conventional requirement imposed on the control signal response, as it used to create the image of the characterized surface.

1 Introduction

The use of two actuators to control a single position variable is usually introduced to simultaneously achieve high bandwidth, range, and precision in following a prescribed trajectory. Usually a long range actuator is assisted with a fine positioner to improve over its accuracy and/or bandwidth. For Example, a voice coil actuator is used to perform most of the travel range required and a piezoelectric actuator with a few micrometers of range is used to achieve nanometer positioning precision. This particular example is commonly observed in hard disk drive systems. In order to achieve nanometer precision, solid-state actuators such as piezoelectric, electrostricitve, and magnetostrictive actuators are commonly used. The positioning resolution for such actuators is usually limited by sensor, amplifier, and control system noise floor. Travel range in these actuators is limited by the maximal allowable material strain in response to a given electric field or magnetic field. In such actuators larger displacements require larger actuator lengths, in the direction of travel. This consequently leads to lower resonances of these actuators.

In nano-positioning systems, feedback control is usually used to achieve higher repeatability than open loop control. Dual actuated systems with a single measurement are dual-input-single-output (DISO) control systems. The controller design for such systems is much more challenging than single-input-single-output (SISO) systems due to the coupling between the choice of control for each actuator and the overall system behavior. Recent reviews of controller design aspects in such systems can be found in [9, 10].

The atomic force microscope (AFM) has become a very popular tool in research and industries of Nanotechnology, Bio-technology, MEMS, and life sciences. The AFM has been primarily actuated by piezoelectric tube actuators. However, the system bandwidth has been found to be significantly lower than the actuator's open loop resonance. PID controllers are commonly used in AFM systems to facilitate on-line tuning of the controllers along with changes in sample-probe combinations. More recently an H_∞ controller synthesis has been used [5] to design a controller based on an experimentally identified model of the piezotube dynamics. As reported by the authors, their control implementation lead to five times faster scanning speed than obtained using a PID controller. However, this was at the expense of the control signal containing significant oscillations. As the control signal is used to create the image of the scanned surface, the image was not representative of the actual sample.

Meanwhile, a piezoelectric film has been patterned onto cantilevers, see for example [6], allowing for an alternate actuation scheme. The use of self-actuated micro-cantilevers has been found to offer performance enhancements yet at the expense of a small allowable travel range. These results suggested use of dual actuation as the natural solution. In this context, a thermal actuator in [7] and a piezotube in [8] have been combined with a piezoelectric cantilever to scan a selected sample. In these efforts, it has been demonstrated that range beyond that of the fine actuator can be achieved via the additional actuator. However, the important question of whether an improvement in the dynamics performance would be achieved with dual actuation over single actuation has not been answered. This paper aims to answer this question.

2 AFM Systems

The basic principle of the AFM operation is based on using a micro-cantilever with a sharp object at its tip to probe a scanned surface. The cantilever is mounted on

a piezoelectric tube scanner, which can translate both laterally and vertically, see Figure 1. Lateral scanning is performed via the piezotube actuator with a prescribed scan size and rate. As the probe touches a feature on a surface, it generates a force causing the cantilever to deflect. Therefore, light from a laser source reflects off the cantilever's tip and the corresponding change in cantilever deflection is recorded via a position sensitive split photodetector (PSD). This sensor measurement is then compared to a chosen setpoint detector voltage, reflecting a nominal setpoint cantilever deflection. The difference between the current sensor output and nominal output is then sent to a controller. The controller causes a piezoelectric actuator to extend or retract via an input voltage in order to maintain the nominal detector setpoint. This actuator is either the piezotube actuator or the self-actuated piezocantilever. This is referred to as contact mode AFM. Whereas, tapping mode AFM is similarly operated but rather with intermittent contact with the sample. This is achieved by driving the cantilever through a harmonic excitation near its resonant frequency. In this case, piezoelectric actuation is used to maintain a constant root-mean-square (RMS) cantilever deflection.

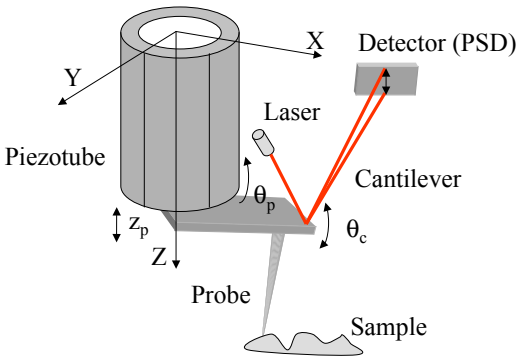

Figure 1: Principle of AFM operation.

3 AFM Dynamical Model

In this a section, we extend our earlier model to span different actuation configurations and operating modes. A brief explanation of the model will follow, for details see [4, 1, 2, 3]. The system's dynamics of interest are characterized by three degrees-of-freedom: z_p the extension of the piezotube, θ_p the piezotube bending, about the Y-axis in Figure 1, and θ_c the cantilever bending relative to the tube base. These are the only degrees-of-freedom of interest in terms of the vertical dynamics. In AFMs, the control action is concerned with the vertical and not the lateral dynamics of the scanner. The lateral motion, i.e., the scanning, is prescribed by the choice of the scanned spot size and the sampling resolution via open loop input voltages. Though it is desired that the tube only extends or retracts to a given voltage, this ideal behavior is not achieved in practice. A small piezotube bending in response to this input voltage is usually observed due to inevitable tube eccentricity. Therefore, it is necessary to include the bending of the tube θ_p as it affects the cantilever bending dynamics. Coupling between extension and bending dynamics of piezotube scanners used in AFMs was first reported in [3]. Equations (1-4), govern the system dynamics of interest. Here, the first three equations describe the dynamics of each DOF and the fourth equation is the measurement.

$$\begin{aligned}
\theta_c(s) \;\approx\; & \sum_{i=1}^{i^*} \frac{(a_{2zi}s^2 + a_{1zi}s)}{s^2 + 2\zeta_{ci}\omega_{ci}s + \omega_{ci}^2}\, z_p(s) \\
& + \frac{(a_{2\theta i}s^2 + a_{1\theta i}s)}{s^2 + 2\zeta_{ci}\omega_{ci}s + \omega_{ci}^2}\, \theta_p(s) \\
& + \frac{a_{fi}}{s^2 + 2\zeta_{ci}\omega_{ci}s + \omega_{ci}^2} f_c \\
& + \frac{k_{\theta ci}}{s^2 + 2\zeta_{ci}\omega_{ci}s + \omega_{ci}^2} u_2 \\
& + \frac{a_{bi}}{s^2 + 2\zeta_{ci}\omega_{ci}s + \omega_{ci}^2} f_b \qquad (1) \\
\theta_p(s) \;\approx\; & \sum_{j=1}^{j^*} \frac{k_{\theta pj}\, u_1}{s^2 + 2\zeta_{\theta p_j}\omega_{\theta p_j}s + \omega_{\theta p_j}^2} \qquad (2) \\
z_p(s) \;\approx\; & \sum_{m=1}^{m^*} \frac{k_{z_p m}\, u_1}{s^2 + 2\zeta_{z_p m}\omega_{z_p m}s + \omega_{z_p m}^2} \qquad (3) \\
y_m \;=\; & \theta_p + \theta_c \qquad (4)
\end{aligned}$$

i^*, j^*, and m^* are the number of modes considered for each degree-of-freedom, ζ is damping ratio, and ω is natural frequency. External inputs u_1 and u_2 are input voltages applied to the piezotube and piezocantilever, respectively. In Equation (1), f_b is a harmonic bimorph excitation used in tapping mode AFM to drive the cantilever near it's 1^{st} resonance. Whereas, f_c is the probe-surface interaction force, which is simply the contact force in contact mode. This probe-sample force is a nonlinear function of the relative position between the probe and the contacted surface. In this regard, changes in this force along with scanning, including any nonlinearities, will be represented as an external disturbance d_c. This disturbance accounts for changing the cantilever deflection during scanning. The following approximation of the probe-surface force will be used, where c_1 and c_2 are constants:

$$f_c \approx c_1\theta_p + c_2 z_p + d_c \qquad (5)$$

The following relation between the detector output y_m, input voltages u_1 and u_2, the biomorph excitation f_b, and the topography induced disturbance d_c may be deduced from Equations (1-4):

$$y_m = P_1 u_1 + P_2 u_2 + W_d(\alpha_1 d_c + \alpha_1 f_b) \qquad (6)$$

Where $P_1(s)$, $P_2(s)$, and $W_d(s)$ are appropriate transfer functions, which depend on the number of modes included from each degree-of-freedom and α_1 and α_2 are scalar gains. $P_1(s)$ is a $2(i^* + j^* + m^*)^{th}$ order transfer function, with relative degree two. The poles are those corresponding to all of included modes. Whereas, $P_2(s)$ and $W_d(s)$ are transfer functions of order $2i^*$ of relative degree two. In here, the poles are those of the cantilever bending modes. Experimental frequency response results of AFM dynamics have been reported in earlier efforts [1, 2, 6]. Typical values of piezotube bending, piezotube extension, and cantilever bending 1^{st} resonances are of the order of few hundred Hz, few kHz, and tens of kHz, respectively.

4 AFM Control Problem

4.1 System Set-Up

The task of AFM control system in contact (or tapping) mode is to reject the effect of variations in the scanned surface on maintaining probe-surface contact (or intermittent contact). This is verified by maintaining a constant setpoint detector output (or constant RMS detector output). The height of the contacted surface at each scanned point is given by the product of the control voltage sent to the actuator at this point and the calibrated sensitivity of the actuator in nm/volts. In dual actuation, each control voltage is scaled by the corresponding actuator's sensitivity and the sum is used as an image.

Figure 2 shows the two signals of interest recorded during a selected AFM scan. The scan is made for a triangular silicon grating with an included angle of about 70°. Figure 2(a) shows the sample's height along a scanned cross section, i.e., the control signal scaled by the actuator's voltage-displacement sensitivity. In addition, the deflection (error) signal is given in Figure 2(b). This signal is the difference between the detector's output and the setpoint output.

The block diagram representing the dual actuator AFM system is given by Figure 3. In this scenario, the piezotube and a piezocantilever are supplied with input voltages u_1 and u_2, respectively. The control action associated with each actuator input is represented by the controller transfer functions $C_1(s)$ and $C_2(s)$. Here, it is desired to maintain the output of the detector, y_{PSD},

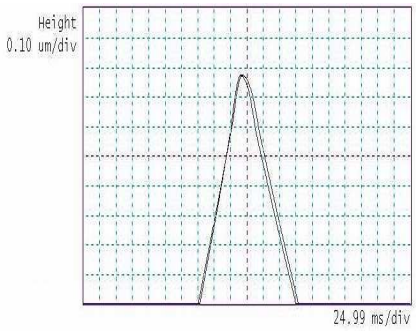

(a)

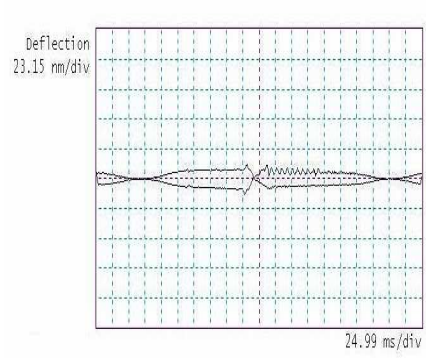

(b)

Figure 2: Experimental AFM signals: (a) control (height) signal, (b) error (deflection) signal.

at the nominal setpoint voltage, r or correspondingly the RMS value in tapping mode. In the block diagram, n represents measurement noise for the PSD sensor, which is dominated by shot noise and noise from the sensor's electronics. Note that $d = (\alpha_1 d_c + \alpha_1 f_b)$.

An important notion here is that of the scanning induced disturbance, d_c. This disturbance frequency is proportional to the scanning speed (prescribed by the user's choice of scan rate and scan size) and inversely proportional to the scanned surface's wavelength. An important distinction between contact and tapping mode takes place. In both situations, the feedback bandwidth is actually the same but the speed of scanning is quite lower in tapping mode. This is the case since scan speed will also depend on the speed of the response of the cantilever's oscillation in tapping mode.

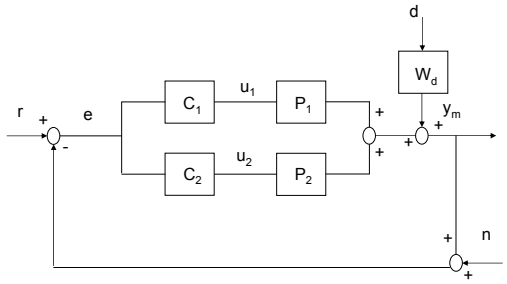

Figure 3: Block diagram of AFM dual actuator configuration.

4.2 Feedback Structural Limitations

The response of the control (image) and error (deflection) signals to the scanned surface variations, i.e., output disturbance, is governed by the control sensitivity S_u and the output sensitivity S_o functions, respectively. In feedback systems, the control sensitivity and output sensitivity functions are defined as follows:

$$S_u = \frac{u}{-d} \quad , \quad S_o = \frac{e}{-d} \tag{7}$$

Naturally the sensitivity function, S_o, is desired to be of a small gain at low frequencies up to a maximal possible bandwidth for good disturbance rejection. However, in AFMs an additional requirement is imposed on the control response. It is desired that the frequency response of the control sensitivity function be flat up to a maximal possible frequency. This leads to the control signal being representative of the disturbance created by scanning. This is required because the control signal is used to create the image of the scanned surface. If this is simultaneously achieved with the small error requirement on S_o, an accurate image of the scanned surface is recorded. However, these objectives are coupled, with the coupling taking the following form in single and dual actuation, respectively.

$$S_o = W_d - PS_u \tag{8}$$

$$S_o = W_d - P_1 S_{u1} - P_2 S_{u2} \tag{9}$$

This naturally suggests that for good disturbance rejection, $S_u \approx P^{-1}W_d$ within the frequency range of operation. This suggests that the product $P^{-1}W_d$ does not permit an arbitrary shape of the response of an actuator input voltage to the topography induced disturbance. A particularly troublesome notion comes from the plant's open loop zeros since they become resonances of the control sensitivity. This leads to oscillations in the control signal used, which are not due to the scanned surface. This can be seen from the interpolation constraint $S(z) = 1$ on the $j\omega$-axis, where z is an open loop zero. A small $|S(j\omega)|$ near the frequency of plant zeros requires dS/ds large and positive near this frequency. This leads to degrading the control response via a large peak in $S_u = CS$, unless the controller gain is sufficiently small near this zero frequency.

The extent of these image corrupting phenomenon is further aggravated due to the fact that open loop poles and zeros in these systems are typically lightly damped. Figure 4 is a sample AFM scan showing an image corruption with control oscillations that are not due to the sample's topography.

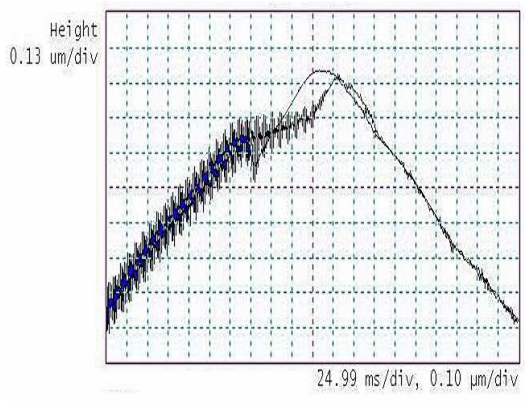

Figure 4: Experimental demonstration of image oscillations due to piezotube actuator dynamics.

In the dual actuation, the sum $u_1 + u_2$ is responsible for rejecting the full disturbance. The main advantage is seen from the fact that plant dynamics cancelled in the branch $C_i P_i$ will not appear as a pole or a zero of the control sensitivity associated with the other controller. This is contrasted with the SISO situation, where inverting the dynamics automatically leads to a control (image) altered by the system's dynamics. This leads to requiring that S_{u1} contains the dynamics of $P_1^{-1}W_d$ even beyond roll-off of the piezotube actuator. Otherwise, the dynamics in P_1 will appear in S_{u2}. As a result, the image will be corrupted since it is created from both control voltages u_1 and u_2. This limitation is typically not a concern in most dual actuated systems.

4.3 System Uncertainty

In atomic force microscopes, changes in the cantilever-probe assembly and the force setpoint are the main source of uncertainty. In this regard, changes in the cantilever or sample lead to changing the effective stiffness and damping of the cantilever viewed at the output. This effective stiffness is also dependent on the

force setpoint to be maintained. This is the case as the effective surface stiffness varies nonlinearly with interaction force. This, in turn, leads to changing the poles associated with the cantilever modes, the anti-resonances of the coupling between the cantilever and the piezotube, and correspondingly the system's DC gain. Experimental demonstrations of such uncertainties may be found in [2].

5 Design Example

In this section, a sample experimentally identified model is used for controller design demonstration. Here, the 1^{st} piezotube bending resonance is at about 400 Hz and an anti-resonance at 550 Hz with damping ratios both approximately of 0.1. The 1^{st} extension mode resonance and anti-resonance are at 4.6 kHz and 3.5 kHz, respectively, with damping ratio of 0.1. Finally, the cantilever bending mode resonance is at 50 kHz with a damping ratio of about 0.05, this is the highest frequency mode included. In this regard, an H_∞ controller synthesis is used to demonstrate that such limitations are independent of the algorithm used.

First, the single actuator, with a piezotube, system is considered. This is achieved by letting $u_2 = 0$ in Equation 6. Figure 5 shows the frequency response with an 8^{th} order controller, designed via an H_∞ synthesis. Here, a bandwidth of about $200Hz$ is achieved while maintaining an acceptable control response. Yet pushing the bandwidth further inevitably leads to a control sensitivity peak at about $6dB$, which is around $500Hz$ the frequency range of the 1^{st} piezotube bending mode. This peak corresponds to an overshoot of about 20% in the control signal response to step change in the topography induced force disturbance. The step response of the control signal for both designs of Figure 5 are contrasted in Figure 7 (a). Such peaks in the control sensitivity are responsible for oscillations in the image as those in Figure 4.

Next, the dual actuated situation is contrasted with the piezotube actuated system. Here, the relative range of actuators is important. A typical design objective in a dual actuation scenario as this one is that S_{u1} would be of a large gain but low bandwidth. While for the fine actuator, S_{u2} is of lower gain but higher bandwidth. . This is attributed to the fact that the input range available to the each actuator relative to the total size of the disturbance is different. In here, the ratio of S_{u1}/S_{u2} static gains will be designed to be about 5-6. This is in accordance with typical travel ranges of $3-5\mu m$ for the piezotube and $.5-1\mu m$ for the piezocantilever. The combined action of both actuators should reject the full disturbance at steady-state.

In Figure 6(b), the lower gain control sensitivity, S_{u2},

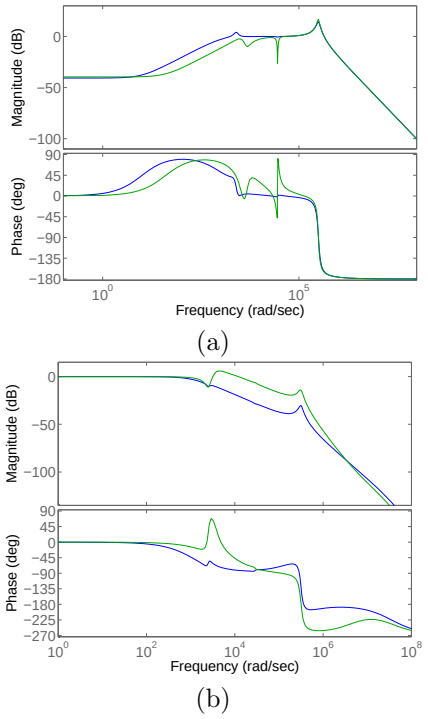

Figure 5: Bode diagrams for piezotube actuation : (a) sensitivity, (b) control sensitivity.

displays a flat response near the piezotube modes. This is made possible by use of controller C_1 that inverts all the dynamics of P_1 even those within a frequency beyond the roll-off of the piezotube actuator. Figure 7(b) shows the response of both control signals to a step change in the topography induced disturbance. It is clear that the sum of a fast but small range signal (u_2) and a larger range but slower signal (u_1) add to one to cancel the unit step disturbance. In this situation, dual actuation can be used to improve over single actuation. However, the existence of several plant poles and zeros in the frequency range between the piezotube bandwidth and the fine actuator bandwidth is a challenge, see for example [2]. Therefore, a controller C_1 needs to cancel the poles and zeros of the 1^{st} piezotube extension mode as well as those of the 2^{nd} piezotube bending and extension modes. Otherwise, any of these lightly damped modes, in P_1 will appear in the control response of the piezocantilever and thus corrupt the recorded image. This appears as practically difficult to sustain especially along with system uncertainty. An even moderate uncertainty that does not affect stability or degrade performance can lead to corrupting the control response, and thus the targeted image.

6 Conclusions

In this effort, the problem of dual actuation in AFMs has been addressed. The fact that the control signals

are used to create the scanned surface's image introduces a significant challenge. This requires that both control signals used to actuate a piezotube and a piezocantilever need not to be altered by both plant transfer functions. Fundamental characteristics of feedback systems suggest that though an improvement in performance is possible with dual actuation, the conditions required to obtain this improvement are practically unachievable.

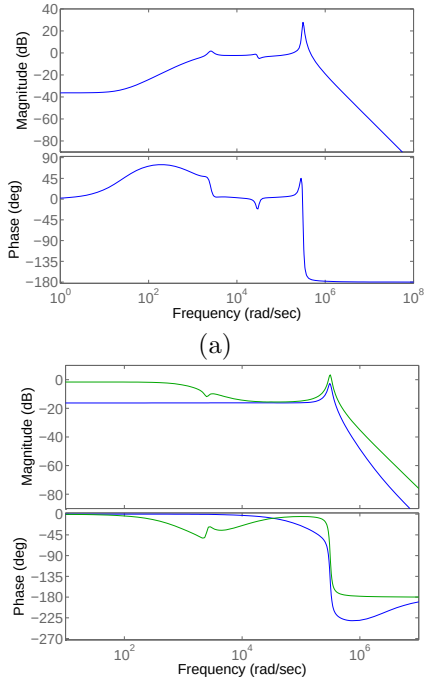

Figure 6: Bode diagrams for dual actuation : (a) sensitivity, (b) control sensitivity.

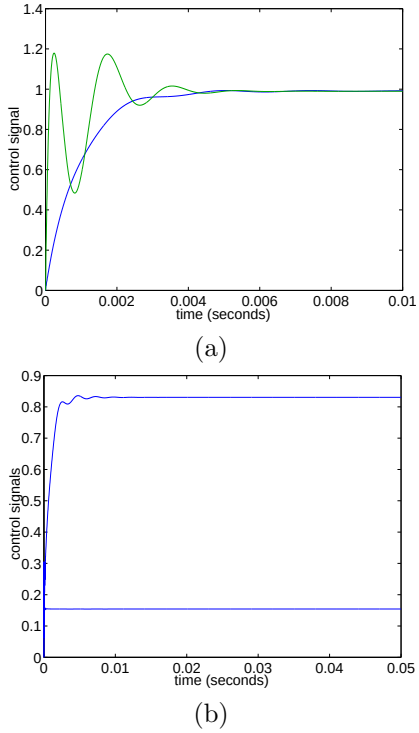

Figure 7: Control signal(s) response to a step disturbance for :(a) single actuation, (b) dual actuation

References

[1] O. M. El Rifai, and K. Youcef-Toumi. Trade-offs and Performance Limitations in Atomic Force Microscope Feedback System, *IFAC Conference on Mechatronic Systems*, Berkeley, CA, December 2002.

[2] O. M. El Rifai, and K. Youcef-Toumi. Dynamics of Atomic Force Microscopes: Experiments and simulations, *IEEE Conference on Control Applications*, Scotland, September 2002.

[3] O. M. El Rifai, and K. Youcef-Toumi. Coupling in Piezoelectric Tube Scanners Used in Scanning Probe Microscopes, *American Control Conference*, Arlington, VA, pp.3251-3255, June 2001.

[4] O. M. El Rifai, and K. Youcef-Toumi. Dynamics of Contact-mode Atomic Force Microscopes, *American Control Conference*, Chicago, IL, pp.2118-2122, June 2000.

[5] G.Schitter, P.Menold, H.F. Knapp, F.Allgower, and A.Stemmer. High Perfromance feedback for fast scanning atomic force microscopes. *Review of Scientific Instruments*, **72**(8), August 2001.

[6] T. Sulchek, G.G. Yaralioglu, C.F. Quate, and S.C. Minne. Characterization and optimization of scan speed for tapping-mode atomic force microscopy. *Review of Scientific Instruments*, **73**(8), August 2002.

[7] T. Sulchek, S.C. Minne, J.D. Adams, D.A. Fletcher, A. Atalar, C.F. Quate, and D.M. Adderton. Dual integrated actautors for extended range high speed atomic force microscopy. *Applied Physics Letters*, **75**(11), September 1999.

[8] A. Egawa, N. Chiba, K. Homma, K. Chinone, and H. Muramatsu. High-speed scanning by dual feedback control in SNOM/AFM *Journal of Microscopy*, **194** , pp.325-328, May/June 1999.

[9] J. Ding, M. Tomizuka, and H.Numasato. Design and Robustness Analyis of Dual Stage Servo Systems, *American Control Conference*, Chicago, IL, pp.2605-2609, June 2000.

[10] S.J.Schroceck and W.C. Messner. On Controller Design for Linear Time-Invariant Dual-Input Single-Output Systems, *American Control Conference*, San Diego, CA, pp.4122-4126, June 1999.